Inelastic energy loss and charge exchange in low-energy heavy ions scattered from Cu and Cu-alloy surfaces

Ting Li and R. J. MacDonald
Department of Physics, The University of Newcastle, Callaghan, New South Wales 2308, Australia
(Received 11 October 1994)

Inelastic energy loss and charge exchange processes in low-energy (1–9 keV) Ne^+ ions scattered from the Cu atoms in Cu(100), $Cu_3Au(100)$, and polycrystalline Cu surfaces have been studied at large scattering angles. The experiments reveal that significant inelastic energy losses (up to 300 eV) occur in these scattering systems. The inelastic energy loss observed is independent of the Cu target matrix. It shows a sharp increase with increasing incident energy at a threshold energy dependent on the scattering angle. The scattered Ne^+ ion yield, the Ne^{2+} ion yield, and the Cu^+ recoil yield all show a similar threshold-type behavior as a function of incident energy. The threshold energies vary as a function of scattering angle. Various theoretical models of inelastic energy loss are discussed but the experimental results in general do not agree with these models. A model is suggested in which the total inelastic energy loss is proposed to be composed of two parts: the energy lost in continuous electron excitation along the incoming and outgoing trajectories and the energy lost in the inner-shell electron promotion during close atomic encounters. Good agreement between experiments and the model is obtained. The inelastic energy loss in Na^+-Cu and Ne^+-Au collisions was also studied and compared with that of Ne^+-Cu collisions. Charge exchange in these inelastic energy-loss processes is discussed.

I. INTRODUCTION

An ion colliding with atoms on a surface loses energy by the elastic collisions of the nucleus and by the inelastic interaction of the electrons. Electron interaction results in charge-transfer processes such as neutralization, ionization, and reionization of the incident ion. Inelastic energy loss and charge-exchange mechanisms are the most important factors limiting the understanding and quantitative interpretation of low-energy ion-scattering spectroscopy (ISS). Extensive studies[1–8] have been focused on the charge exchange or neutralization process due to its importance in the quantification of analytical techniques such as ion scattering or secondary-ion-mass spectroscopy. Less work has been done on inelastic energy loss. Although inelastic energy losses are usually small at the energies which are mainly used in surface scattering experiments, the processes involved in inelastic energy loss play an essential role in the ionization and electron emission processes accompanying the ion scattering, and determine to a considerable extent the charge composition of scattered particles. Charge exchange and energy loss are interrelated, and understanding the ion-surface interaction requires that both processes themselves be understood.

The theories of the inelastic energy loss were mainly developed by Firsov[9] and Lindhard and Scharff.[10] Both theories are based on the Thomas-Fermi model of the atom, and yield the same relation between energy loss and ion velocity. If limited to the case of small scattering angles, and if the atomic numbers of the colliding particles differ by no more than a factor of 4, Firsov[9] derived a formula which suggested that the fraction of the kinetic energy lost in the inelastic processes is proportional to the velocity of the atomic particle and is a monotonically increasing function of the atomic numbers Z_1 and Z_2 of the collision partners. Later, Oen and Robinson[11] developed a semiempirical approach to the inelastic loss for light projectiles, in which the spatial dependence of the inelastic loss was chosen to follow approximately the electron density around the target atoms. Kishinevsky and co-workers[12–14] also derived an expression for inelastic energy transfer in terms of the relative atomic velocity and energy for the case of two arbitrary atoms and for any impact parameter. Recently, stopping-power theory in general[15] has been extended to surface scattering processes.[16,17] The inelastic energy loss was found to be proportional to the particle trajectory length and the velocity of the incident particle for light projectiles at grazing angle incidence to a solid surface. In all these studies, the inelastic energy loss is given as a continuous function of the projectile velocity (or incident energy) and the distance of closest approach (or impact parameter).

Direct measurement of small inelastic energy losses in low-energy ion scattering from solid surfaces is complicated by difficulties associated with the calibration of the analyzer and the accurate alignment of the system,[18] as well as by difficulties with accurate measurements of the incident ion energies. Multiple-scattering effects and the scattering of incident particles scattered from deeper layers also influence the measured scattered energy position relative to the predicted energy of elastically scattered ions involved in binary collisions. Inelastic losses of low-energy ions scattered from solid surfaces have been observed as displacements of the measured scattered ion energy from the position of the binary elastic collision event. The inelastic energy losses of low-energy (below 2 keV) He^+ ions scattered from solid surfaces at large

0163-1829/95/51(24)/17876(15)/$06.00

scattering angles have been measured and compared with the Oen-Robinson and Firsov models.[19–22] Qualitative agreement between experiments and theories was obtained. Studies of the inelastic energy loss and charge-exchange processes in low-energy (below 10 keV) light projectiles (He, H) scattering from solid surfaces at grazing angle incidence suggested that a large number of electron-hole pairs can be excited, causing significant inelastic energy losses.[16,17] The Firsov or Lindhard formulation has often been used to model the inelastic energy loss in computer simulations.[23–25] Significant departures of the scattered energy position from those predicted by elastic scattering of Ne^+ from the Ag surface were observed at large scattering angles.[26] The energy losses were suggested to be path length and impact parameter dependent. However, direct experimental tests of these inelastic loss theories at low ion energies have not been very successful, owing to the experimental difficulties encountered.[27]

Studies of Ne^+ ions scattered from Mg, Al, and Si surfaces[28–32] suggested that electron promotions during close encounters are significant in keV ion-surface collisions. The projectile excitation was observed to be very similar to that observed in gas-phase processes.[33–35] Inelastic energy losses of about 45 eV were observed for Ne^+ scattered from the Mg surface, in agreement with the electronic energy required to form doubly excited Ne^{**} states.[28] Studies of charge fraction and inelastic loss processes of several ion-target combinations also suggested that the occurrence of reionization processes in keV energy regions could be associated with observed energy loss.[36,37] The mechanism was suggested to involve level promotion and crossings[38–40] within the collision partners, i.e., it is related to the electron shell structure of the atoms. The occurrence of such inner-shell electron excitations make the study of inelastic loss in low-energy ion-surface interactions difficult. In gas-phase collision events, several distinct peaks induced by different inner-shell electron excitation processes are often observed in the scattered ion energy spectra.[33] In the case of the ion-surface scattering, these peaks are not resolved in the scattered ion energy spectrum[28,32,41–45] due mainly to two reasons: (1) the broadening of the spectrum caused by quasisingle (QS) (Ref. 42) or multiple-scattering events resulting from the close proximity of other atoms in the solid target, or (2) the smaller energy difference between these peaks because shallower electron shells are usually encountered at the lower incident energies used. Further, in the case of solid surface targets, projectile outer-shell electrons can be excited during the pass through the surfaces, which may effect the excit channels of inner-shell electron excitations.[39,40]

An anomalous increase of the ion fraction with the increasing incident energy was observed above 7 keV for Ne^+ off a Cu(100) surface at a scattering angle of 30° in the later 1970s.[41,42] At large scattering angles, 5–6-keV Ne^+ ions were found to be well suited for low-energy ion-scattering (LEIS) analysis of clean and oxygen-covered copper surfaces since the position of the shadow edges were not distorted by neutralization effects. This was in marked contrast to the situation for 2–3 keV Ne^+ ions[43] scattered off the same surfaces. Large displacements of the scattered energy from that predicted by elastic binary scattering theory have been observed for 5-keV Ne^+ scattered from Cu(110) surfaces at a 164° scattering angle.[44] It was suggested that reionization of Ne^+ was a possibility, but the peak displacement observed was about 100 eV, much greater than the first ionization energy of Ne of 20 eV.

More recently Buck *et al.*[45] reported on the difference in the neutralization of 2.4–10 keV Ne^+ ions scattered from the Cu and Au atoms of a $Cu_3Au(100)$ alloy surface using time-of-flight (TOF) spectroscopy. As the incident Ne^+ energy was increased, the ion fraction of Ne^+ scattered from Cu atoms was found to exhibit a sharp increase at a threshold of 4–5 keV incidence for a scattering angle of 90°. Peak displacements from the elastic binary collision position of up to 130 eV were also observed under the assumption that there was no inelastic energy loss in the Ne^+-Au collisions. The proposition that Ne 2*s* vacancies are formed during the close collisions of Ne and Cu atoms gives a reasonable explanation for the large peak displacements and Ne Auger electron emission results observed, and leads to a further understanding of the charge-exchange process and its correlation with the inelastic energy-loss process in Ne^+ ions scattered from Cu surfaces.

However, due to difficulties in calibrating TOF systems, the calibration of the detector was based on the assumption that there is no inelastic energy loss in Ne^+-Au collisions.[45] This may lead to an underestimate of the inelastic energy loss actually occurring in Ne^+-Cu collisions. Another factor which might also effect the value of inelastic energy loss is that the inelastic energy loss referred to in these papers[44,45] is the difference between the energy calculated from the binary collision model and the energy of the measured scattering peak (the so-called peak shift[44] or peak displacement[45]). The value of the actual inelastic energy loss, which can be obtained using the scattering particle method,[33] is generally larger than that of the corresponded peak shift.

The results of a systematic study of the inelastic energy loss and charge-exchange processes of 1–9-keV Ne^+ and Na^+ scattered from Cu(100), $Cu_3Au(100)$ and Cu polycrystalline surfaces are reported in this paper. The influence of structure, target matrix, and scattering geometry on the inelastic processes were also studied. Large scattering angles were used to minimize multiple-scattering effects.[46] Careful calibration of the system was performed. Inelastic energy losses were obtained using the scattered particle method,[33] and compared with corresponding peak displacements at different scattering geometries. The scattered Ne singly and doubly charged ion yield and Cu^+ positive recoil yield were also measured as a function of incident energy. Inelastic energy losses of Na^+-Cu and Ne^+-Au collisions were measured and compared with those of Ne^+-Cu collisions. Various models which have been used to explain inelastic energy losses are discussed and compared with the experiments. A model is proposed which suggests the inelastic energy loss is composed of two parts: the energy lost in electron excitation along the incoming and outgoing trajectories,

and the energy lost in an inner-shell electron promotion during close atomic encounters. Charge exchange in these inelastic energy-loss processes is also discussed.

II. EXPERIMENTS

The experiments were performed in a Leybold-Heraeus ion scattering system. A base pressure of 5×10^{-11} mbar was achieved by using a turbomolecular pump in combination with a titanium sublimation pump. The equipment used in these experiments has been described previously.[4,20,26]

Careful energy calibration of the system was performed by introducing the ion beam directly into the electrostatic energy analyzer. The scattering angle is defined to better than $\pm1°$.[26] Two different electrostatic energy analyzers were used in the study: a 0–2-keV analyzer in the $\Delta E/E$ constant mode and a 0–10-keV analyzer in the ΔE constant mode. Results obtained using these two different analyzers overlap within experimental errors, producing an independent check of the energy calibration of the system.

The measurements were performed using a variety of experimental conditions, over a significant period of time, in order to avoid possible systematic errors. The experimental errors for the scattered ion energy derived from these experiments amount to less than 1% of the measured value.

Samples were cleaned by 2-keV Ar^+ bombardment, followed by annealing at temperatures above and below 390 °C [the order-disorder critical temperature of $Cu_3Au(100)$]. This bombardment and the annealing cycles were repeated until a clean [and well ordered for Cu(100) and $Cu_3Au(100)$] surface was obtained. The composition and structure of $Cu_3Au(100)$ have already been reported,[24,25] and will not be described here.

The software package GRACES, which is a program originally written for Rutherford backscattering (RBS) simulation and data analysis,[47] was modified and used to analyze the experimental spectra. The data analysis functions in this program (background subtraction, curve smoothing, region of interest integration, spectrum conversion from $\Delta E/E$ constant to ΔE constant mode, nonlinear curve fitting with various functions, maximum point reading, etc.) made the analysis of the experimental data very direct and straightforward.

III. EXPERIMENTAL RESULTS

A. Inelastic energy losses

Q, the inelastic energy loss in the collision is defined as[33]

$$Q=E_0-(E_1+E_2)\ , \tag{1}$$

where E_0 is the kinetic energy of incident particles, and E_1 and E_2 are the measured kinetic energies of the scattered and recoil particles, respectively. Q may be obtained in at lest three different ways: the recoil-particle method, the coincidence method, and the scattered-particle method.[33] The latter is adopted here.

By means of Eq. (1) and momentum conservation in the collision, the scattered-particle method relates the inelastic energy loss and the measured energy of scattered projectile:

$$Q=2\gamma(E_0E_1)^{1/2}\cos\theta+(1-\gamma)E_0-(1+\gamma)E_1\ , \tag{2}$$

where $\gamma=M_1/M_2$ is the mass ratio between the projectile and the target atom, and θ is the laboratory scattering angle.

The difference between the energy calculated from the binary collision model E_b and the energy of the measured scattering peak E_1 is used to indicate inelastic energy losses in many studies. This is defined by

$$\Delta E=E_b-E_1\ , \tag{3}$$

where E_b is given by

$$E_b=E_0[\cos\theta+(\mu^2-\sin^2\theta)^{1/2}]^2/(1+\mu)^2 \tag{4}$$

for cases where $\mu=1/\gamma>1$. ΔE is then the peak shift or peak displacement.[44,45]

The relationship between ΔE and Q can be derived from Eqs. (2)–(4):

$$\Delta E=E_0\left\{\frac{\mu}{1+\mu}\frac{Q}{E_0}+\frac{2\cos\theta\sqrt{\mu^2-\sin^2\theta}}{(1+\mu)^2}\left[1-\left[1-\frac{\mu}{(1+\mu)(\mu^2-\sin^2\theta)}\frac{Q}{E_0}\right]^{1/2}\right]\right\}. \tag{5}$$

In the case of no inelastic loss ($Q=0$), there will be no peak displacement ($\Delta E=0$). In most cases, ΔE is not equal to the inelastic energy loss of the collision system, and therefore cannot be used to represent the inelastic energy loss of the system quantitatively. At a scattering angle of 90°, the relation between these two quantities becomes very simple:

$$\Delta E=Q/(1+\gamma)\ \text{ or }\ Q=(1+\gamma)\Delta E\ . \tag{6}$$

In the case of Ne^+ incident on Cu, where $\gamma\approx\frac{1}{3}$, ΔE differs from Q by approximately $\Delta E/3$ when $\theta=90°$.

The scattering geometry used in the experiments for Cu(100) and $Cu_3Au(100)$ surfaces are described below.

(1) A 45° incident angle along the [100] azimuth, and a scattering angle of 135° or 90°. Using these scattering geometries, the scattered ions come mainly from the first layer of the crystal as a result of surface atoms shadowing and blocking deeper layers. This is defined by [100]135° or [100]90°.

(2) A 35° incident angle along the [110] azimuth, and a scattering angle of 135° or 90°. Using these scattering geometries, ions scattered from the second layer have about an equal possibility to be detected as those scattered from the first layer if they can escape without neu-

tralization. This is defined by [110]135° or [110]90°.

(3) A 45° incident angle along the random azimuth direction, and a scattering angle of 135° or 90°. Random here means the avoidance of low index surface directions. For such a scattering geometry, as well as for scattering from the polycrystalline surface, one cannot restrict scattering only to the top one or two layers as in (1) and (2) above. This is defined by random 135° or random 90°. For the polycrystalline Cu target, we will refer only to the scattering angle.

The incident angle is referred with respect to the target surface, and the scattering angle is referred with respect to the incident-beam direction.

Each experiment was repeated several times. Figure 1 shows typical energy spectra of Ne^+ ions scattered from the Cu(100) surface at a scattering geometry of [100]135° for incident energy from 2 to 6 keV. The peaks located around the E/E_0 value of 0.3 ($E_b/E_0=0.3276$) are the scattered Ne singly charged ions. The small peaks arise from doubly charged Ne^{2+} ions which are produced in the collision and appear at half the energy of the singly charged ions in the electrostatic analyzer.[44] The real energy of Ne^{2+} ions is therefore roughly the same as that of the Ne^+. The peak position of scattered singly charged Ne ions was measured and used to obtain the experimental value of peak displacement ΔE and inelastic energy loss Q using Eqs. (3) and (2).

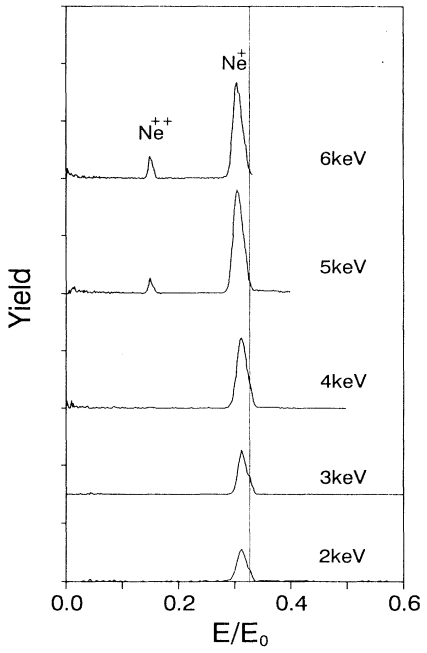

FIG. 1. Typical energy spectra of scattered Ne ions from the Cu(100) surface at [100]135° scattering geometry for an incident energy from 2 to 6 keV. The energy peak positions of scattered Ne^+ ions observed from the experiments are significantly displaced from those predicted by elastic scattering ($E_b/E_0=0.3276$). The small peaks located around the E/E_0 value of 0.15 are due to scattered Ne doubly charged ions.

1. Peak displacements of Ne^+-Cu from three surfaces and the influence of ions scattered from deeper layers

The peak displacements of Ne^+ scattered from Cu in Cu(100), $Cu_3Au(100)$, and Cu polycrystal surfaces were obtained as a function of incident energy using [100]135° scattering geometry. Results are shown in Fig. 2. Experiments performed using geometries which expose only the top layer, top two layers, or deeper layers as in the random or polycrystalline cases gave exactly the same results as these shown in Fig. 2. We note the following features.

(1) Peak displacements of Ne^+ scattered from Cu atoms are the same, within experimental errors, for these three samples.

(2) The peak displacement increases sharply as a function of E_0 at a threshold energy of 3.5–4 keV, and returns to the slower rate of increase at ~6 keV.

2. Peak displacements at different scattering and incident angles

Peak displacements of Ne^+ from Cu in the $Cu_3Au(100)$ surface are compared for different scattering angles at the scattering geometries [100]90° and [100]135° as shown in Fig. 3(a).

Peak displacements of Ne^+ from Cu in the $Cu_3Au(100)$ surface at a 135° scattering angle are also measured for two different incident angles: 45° and 90°. These two scattering geometries reverse the incoming and outgoing trajectories, respectively. The results obtained are the same within experimental errors as shown in Fig. 3(b).

From Figs. 3(a) and 3(b), we can clearly see the following.

(1) In the incident energy range of 1–3 and 7–9 keV, the values of peak displacement for 90° scattering are larger than those for 135°. At about 9-keV incidence this difference is about 100 eV.

(2) The threshold energy for the sharp increase is shifted slightly to higher energy for the 90° scattering than that of the 135° one.

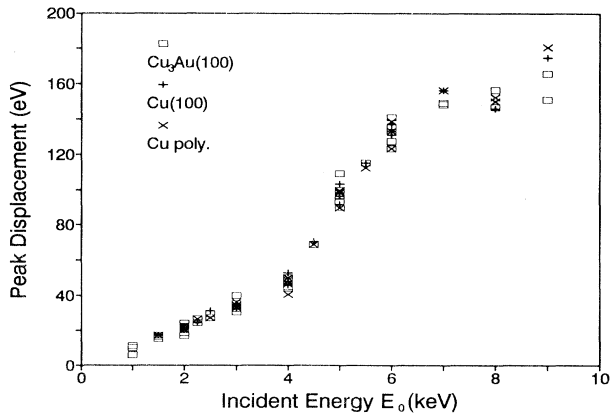

FIG. 2. The peak displacements of Ne^+ ions scattered from Cu atoms in Cu(100), $Cu_3Au(100)$, and Cu polycrystalline surfaces as a function of incident energy at [100]135° scattering geometry.

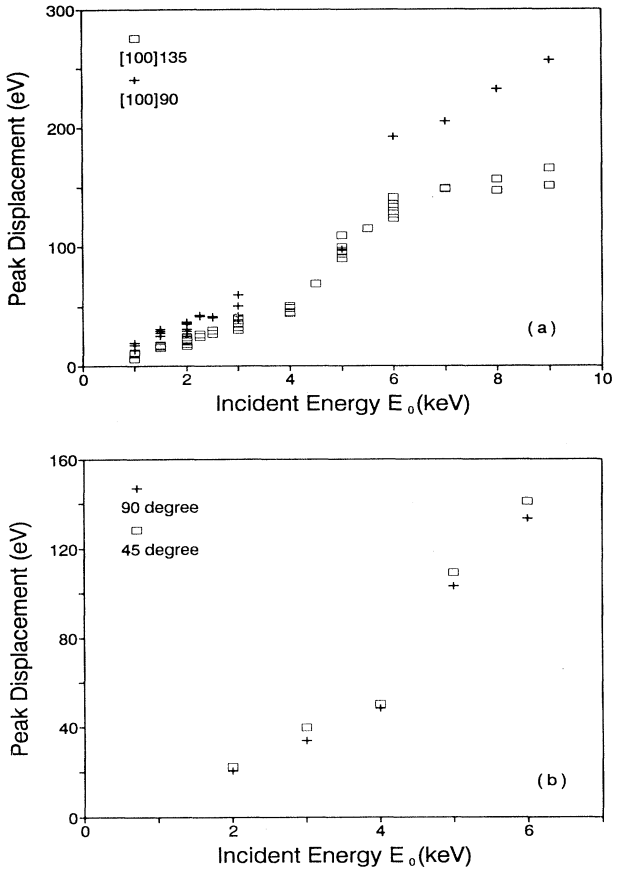

FIG. 3. Peak displacements of Ne^+ ions scattered from Cu atoms in $Cu_3Au(100)$ surface as a function of incident energy (a) for [100]90° and [100]135° scattering geometry and (b) for incident angles of 45° and 90° at a 135° scattering angle.

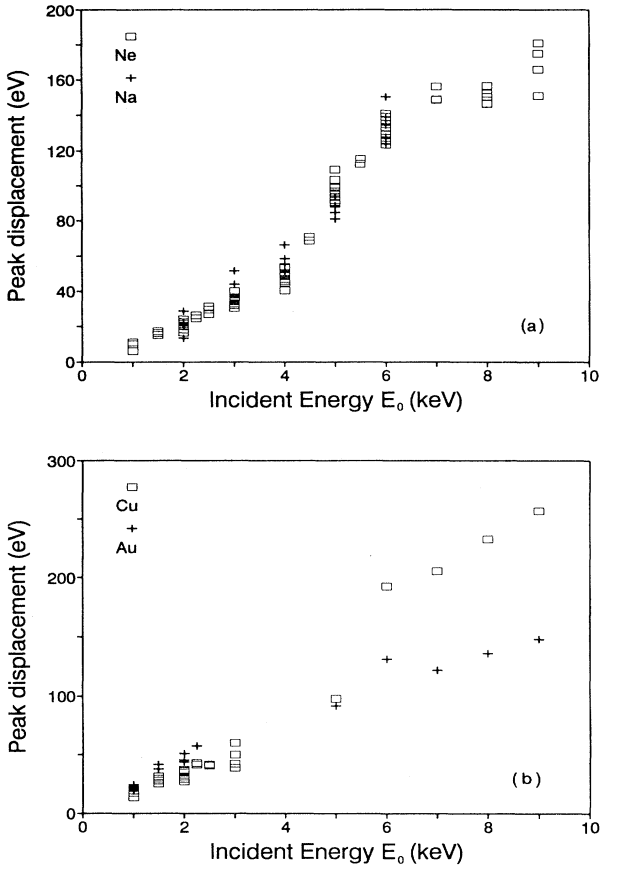

FIG. 4. (a) Peak displacements of Na^+ and Ne^+ ions scattered from Cu atoms in Cu(100), $Cu_3Au(100)$, and Cu polycrystalline surfaces as a function of incident energy at [100]135° scattering geometry. (b) Peak displacements of Ne^+ ions scattered from Au and Cu atoms in $Cu_3Au(100)$ surface at [100]90° scattering geometry.

(3) Within the experimental error, the peak displacements are the same when the incident and exit paths are reversed. The threshold energy is independent of the incident angle to the surface, but does depend on the scattering angle.

3. *Peak displacements of Na^+-Cu collisions*

Peak displacements of Na^+ scattered from Cu in Cu(100), $Cu_3Au(100)$, and Cu polycrystalline surfaces were measured as a function of incident energy using the [100]135° scattering geometry, in the energy region from 2 to 6 keV. The results are independent of the target matrix and behave similarly to those of Ne^+-Cu collisions, as shown in Fig. 4(a). We note that the threshold energy for Na^+-Cu collisions is about 4–5 keV, shifting slightly upwards compared with that of Ne^+-Cu results.

It is well known that the neutralization behaviors near the surface are very different for Ne^+ and Na^+ ions. The results obtained here suggest that the mechanism involved in the inelastic loss leading to this peak displacements is not influenced by the usual different neutralization behaviors.[1,2]

4. *Peak displacements of Ne^+-Au from $Cu_3Au(100)$ surface*

Measurements of the peak shift of Ne^+ from Au collisions in the $Cu_3Au(100)$ surface were also performed using the [100]135° and [100]90° scattering geometries in the incident energy region from 1 to 9 keV. The results show that large peak displacements also exist in the Ne^+-Au scattering events at both scattering angles. Figure 4(b) shows the peak shifts of the 90° scattering case of Ne^+-Au collisions, compared with that of Ne^+-Cu collisions. We note the following.

(1) The peak displacements are larger for the Ne^+-Au collision in the low-energy region (below 3 keV) and much smaller in the higher-energy region (above 5 keV) than that of Ne^+-Cu collisions.

(2) No obvious threshold is observed in Ne^+-Au collisions.

These results indicate that the peak energy position of Ne^+-Cu scattering in the previous TOF measurements[45] were underestimated by 20–150 eV (the value of peak

displacements in the Ne^+-Au collision) depending on the incident energy.

5. *Inelastic energy loss Q*

Using Eq. (2) we obtained inelastic energy losses from the measured scattered energy peak for all the different ion-target combinations and the scattering geometries studied. Figure 5 shows one of the typical results of the inelastic energy loss of Ne^+-Cu collisions at the scattering angle of 135°, in comparison with the corresponding peak displacement. From the results obtained we can conclude that the inelastic energy losses. (1) are larger than that of the corresponding peak shift; (2) have the same threshold energy as that of peak displacements; and (3) show smaller difference in inelastic energy loss than that for the peak shift for different scattering angles. However, the inelastic energy losses are still larger in the 90° scattering case than that of 135° one.

The inelastic energy losses in these scattering systems are large at the scattering angles used. They can be as high as 150 eV for Ne^+-Au collisions and more than 300 eV for Ne^+-Cu collisions at the energies used in these experiments. These results suggest that the usually accepted idea that the energy of the backscattered ions is in agreement with the energy calculated from elastic scattering in low-energy ion scattering experiments[48]—i.e., without invoking any inelastic processes—may need more careful examinations at incident energy above 2 keV or so.

B. Scattered ion yield

1. *Ne single-charged ions*

The measured yield of scattered ions, Y, from atoms on a surface is proportional to the product σP_i, if normalized with respect to primary ion current and equipment factors,[49] i.e.,

$$Y(E_0,\theta) \propto \sigma(e_0,\theta) P_i(E_0,\theta) , \tag{7}$$

where $\sigma(E_0,\theta)$ is the differential scattering cross section for elastic scattering, and $P_i(E_0,\theta)$ is the probability that the ion remains ionized after exiting the surface.

Classical scattering calculations using various interaction potentials indicate that $\sigma(E_0,\theta)$ is a structureless, monotonically decreasing function of primary ion energy, and $P_i(E_0,\theta)$ is characterized as a monotonically increasing function of ion velocity with the form[1,2]

$$P_i(E_0,\theta) = \exp(-v_c/v_\perp) , \tag{8}$$

where v_c is the characteristic velocity,[4,5] and $v_\perp$ is the ion velocity component perpendicular to the surface. This combination would give the ion yield as a function of incident energy as a curve with a broad maximum at some energy of order 1000–2000 eV, followed by a monotonically decreasing yield with increasing energy. The scattered ion yield of the Ne^+-Cu surface as a function of incident energy was known to follow the shape described above in the region below 2.5 keV for 90° angle scattering,[49] the maximum of the scattered Ne^+ yield occurring at about 1-keV incident energy and then followed by a monotonically decreasing yield with higher energies.

The scattered Ne singly charged ion yield (normalized to primary ion-beam current and equipment factors) of Ne^+ from Cu in Cu(100), Cu_3Au(100), and Cu polycrystalline surfaces was obtained as a function of incident energy using the [100]135° scattering geometry for the three targets. The normalized scattered Ne^+ yield using the [100]135° scattering geometry for the Cu(100) surface was also measured. Some of the results are shown in Fig. 6(a). The behavior of the scattered Ne^+ yield shows the following features.

(1) The yield decreases gradually with incident energy in the region below 3 keV, and then shows a sharp increase as inelastic processes contribute.

(2) The threshold for the steep increase is independent of targets and of scattering from deeper layers. The threshold energy is ~3.5 keV for this scattering geometry, which is the same as that for inelastic energy losses.

(3) With an incident energy below the threshold for observation of the sharp increase in inelastic energy loss, Ne^+ ions scattered from second-layer Cu atoms cannot escape without neutralization. This is due to the higher neutralization probability caused by a longer trajectory in the solid than that experienced by ions scattered from the top layer. Above the threshold energy, more and more Ne^+ ions scattered from the second-layer Cu atoms escape without neutralization. At an incident energy of 5 keV, the yield of Ne^+ scattered from the second layer is approximately 80% of the yield from the top layer.

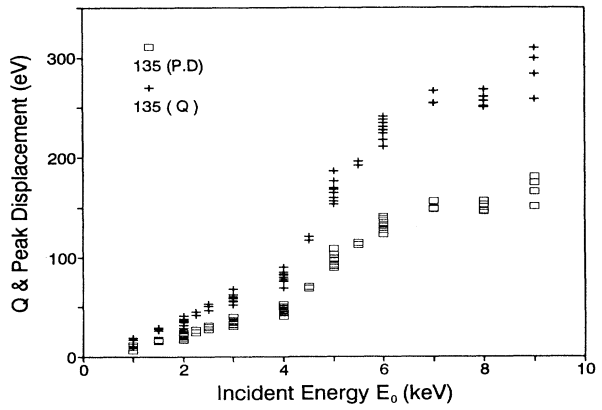

FIG. 5. Inelastic energy losses Q and peak displacements (P.D.) of Ne^+ ions scattered from Cu atoms in the Cu and Cu alloy surfaces at [100]135° scattering geometry.

2. *Ne double-charged ions*

Above 4 keV, Ne doubly charged ions were observed for Ne^+-Cu collisions from all three samples. Measurements of the normalized Ne^{2+} yield as a function of incident energy are shown in Fig. 6(b) using the [100]135° scattering geometry. Figure 6(c) shows the scattered yield ratio of Ne^{2+} to Ne^+ from the Cu(100) surface for both [100]135° and [110]135° scattering geometries. From Figs. 6(b) and 6(c) we see the following.

(1) The 4-keV threshold energy for the formation of Ne^{2+} is independent of samples and slightly higher than that of inelastic energy losses associated with the singly charged ion.

(2) Above the threshold energy, the Ne^{2+} yield increases sharply with increasing incident energy.

(3) The ratio of Ne^{2+} to Ne^{+} yield for the first-layer scattering is about two times larger than that for first two layers. This indicates a preferential charge-exchange process from Ne^{2+} to Ne^{+} or Ne^{0} occurs so that the Ne^{2+} from the second layer cannot leave the surface as a doubly charged states.

(4) At 6-keV incident energy, the yield of Ne doubly charged ions is approximately 10% of that of singly charged ions.

3. *Cu positive recoil*

Direct recoil (DR) atoms constitute a specific case of secondary ions for which the collision energy and DR atom velocity, trajectory, and point of origin are well defined. Hence DR events provide an excellent means for investigation of atom-surface electronic transitions. Such studies are also important for the understanding of inelastic processes in ion-surface collisions that result in conversion of kinetic energy into electronic excitation and ionization energy. The fraction of recoil particles in an ionized state as a result of a specific event is determined by two processes:[50] the close atomic encounter and the outgoing trajectory.

Measurements of Cu positive recoil yield (normalized to the primary ion current and instrumental factor) were performed using the 30° in and 30° out (with respect to target surface) geometry for the Ne^{+}-Cu polycrystalline surface. The yield of Cu^{+} recoil as a function of incident energy is shown in Fig. 6(d). The Cu positive recoil yield rises from a value near zero at about 2 keV, and increases sharply with incident energy.

Errors in the recoil energy peak position are much larger than those obtained from that of scattered ions owing to lower intensity, high background, and broader peak shape. Therefore the inelastic energy obtained from the recoil-particle method and coincidence method were not used to compare with that obtained from the scattering-particle method used in our study.

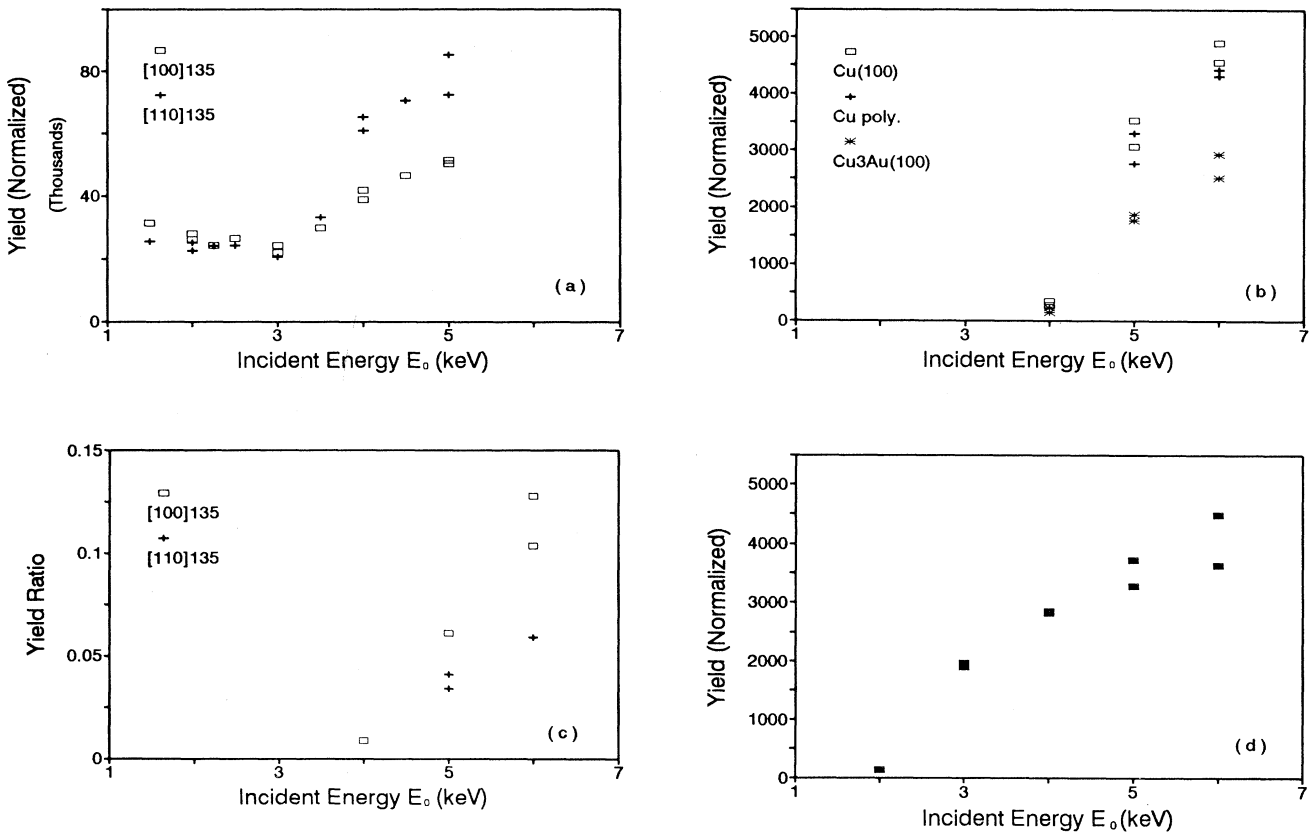

FIG. 6. (a) Scattered Ne^{+} ion yield of the Ne^{+}-Cu(100) surface as a function of incident energy at [100]135° and [110]135° scattering geometries. (b) Scattered Ne^{2+} ion yield of Ne^{+}-Cu atoms in Cu(100), Cu_3Au(100), and Cu polycrystalline surfaces as a function of incident energy at [100]135° scattering geometry. (c) Ratio of scattered Ne^{2+} ion yield and scattered Ne^{+} ion yield of the Ne^{+}-Cu(100) surface as a function of incident energy for [100]135° and [110]135° scattering geometries. (d) Cu^{+} recoil yield of the Ne^{+}-Cu polycrystalline surface as a function of incident energy at 30° incidence and 30° out (with respect to the sample surface) geometry.

C. Summary of experimental results

The experimental results can be summarized as follows.

(1) Inelastic energy losses of Ne^+-Cu surface collisions are independent of the environment of Cu atoms in the targets at the scattering geometries and incident energies studied. Any inelastic loss due to scattering from deeper layers is small compared with inelastic losses in the single collisions. Values of the inelastic energy loss and peak displacement vary as a function of scattering angle.

(2) The threshold energy for sharp changes is the same for the inelastic energy loss and the Ne singly charged ion yield, slightly higher for that of Ne^{2+} yield and lower for that of Cu positive recoil at the given scattering geometry. The threshold energy varies as a function of scattering angle.

(3) The inelastic energy losses of Na^+-Cu collisions behave similarly to that of Ne^+-Cu collisions. The threshold energy is shifted slightly to higher energy for the Na^+ case.

(4) Large inelastic energy losses also exist in the Ne^+-Au collision, but the behavior of the inelastic loss with incident energy is different from that of Ne^+-Cu and Na^+-Cu.

IV. THEORETICAL RESULTS AND DISCUSSIONS

Theoretical studies of the inelastic energy loss of heavy ion-atom collisions at low energies are mainly based on Firsov and Lindhard-Scharff theories. Using the Thomas-Fermi model of the atom, Lindhard-Scharff theory predicted a velocity-proportional electronic stopping at low ion velocities expressed as[10]

$$S_e=\frac{8\pi e^2 a_0 Z_1 Z_2 \xi_e}{(Z_1^{2/3}+Z_2^{2/3})^{3/2}}\frac{v}{v_B}\ , \tag{9}$$

where v_B and a_0 are the Bohr velocity and Bohr radius, respectively. ξ_c is of order of 1–2, but may vary with Z_1 approximately as $\xi_e \approx Z_1^{1/6}$.

If limited to small-angle scattering, and if the atomic numbers of colliding particles differ by no more than approximately a factor of 4, Firsov theory[9] gives

$$Q=\frac{4.3\times10^{-8}(Z_1+Z_2)^{5/3}}{(1+3.1\times10^{7}(Z_1+Z_2)^{1/3}r_0)^5}v_0\ , \tag{10}$$

where Q is the energy loss in eV, v_0 is the velocity of the incident particle in centimeters per second, and r_0 is the distance of closest approach in centimeters.

Without invoking the simplifying assumption of rectilinear and uniform motion of the nuclei, Kishinevsky and co-workers[12–14] derived an expression for the inelastic energy transfer for the case of two arbitrary atoms and for any impact parameter:

$$Q=\frac{0.3\times10^{-7}Z_2(Z_2^{1/2}+Z_1^{1/2})(Z_2^{1/6}+Z_1^{1/6})}{\left[1+\dfrac{0.67Z_2^{1/2}r_0}{a_{TF}(Z_2^{1/6}+Z_1^{1/6})}\right]^3}\times\left[1-\frac{0.68V(r_0)}{E_r}\right]v \tag{11}$$

where v and E_r are the velocity and energy of relative atomic motion, and Z_2 is the greater and Z_1 the smaller of the atomic numbers. r_0 is the distance of closest approach in units of Å. $V(r_0)$ is the interaction potential between the two particles in collision at r_0, and $a_{TF}=0.468$ Å. Q is in units of eV.

To estimate the inelastic energy loss in the scattering of light ions, Oen and Robinson proposed a relation in which the spatial dependence of the inelastic loss was chosen to follow approximately the electron density around the target atoms:[11]

$$Q=(0.45/\pi a_{12}^2)kE^{1/2}\exp(-0.3r_0/a_{12})\ , \tag{12}$$

where $kE^{1/2}$ is the electronic stopping cross section in the low-energy regime. This was chosen such that, at higher energies, when the distance of closest approach r_0 approaches impact parameter b, the full Lindhard-Scharff electronic stopping cross section is retrieved. a_{12} is the screening length in the Molière potential. Although the Oen-Robinson model was initially proposed for light ions, it has been modified in the study of heavy-ion transmission processes.[51]

Recently, the general stopping-power theory,[15] in which the charge state and energy losses caused by the elementary excitations owing to the moving charge traveling in a solid can be understood in terms of the dielectric function of the solid, was extended to surface scattering processes.[16,17] In energy-loss experiments at low energy for light projectiles at grazing angle incidence and small-angle scattering, the trajectory length replaces the foil thickness in a classical energy-loss experiment. The total energy loss in such a process is given by[16,17]

$$Q=\gamma v L\ , \tag{13}$$

where γ is a friction coefficient; v the velocity of the particle; and L the length of the trajectory of the particle, defined relative to some plane above the topmost ion cores of the surface (usually chosen as about half an interlayer spacing of the target). γ and L also vary with incident energy, and thus are a function of particle velocity.

The inelastic energy losses were calculated using Firsov, Kishinevsky-Parilis and Oen-Robinson formula for Ne^+-Cu at scattering angles of 135° and 90°, and compared with those of the experiments. Figure 7(a) shows comparisons of the experimental with the theoretical results for the 135° scattering case. Care must be taken when using these theories, because Firsov's formula is only valid for small scattering angles. The incident velocity and scattered velocity is about the same in the small-angle scattering case. For large scattering angles the incident and scattered particle velocities are quite different. So a modification is made here in using the Firsov formula. By approximately dividing the scattering process into two Firsov processes, the incoming and the outgoing Firsov processes, the velocity term v_0 in the Firsov formula was replaced by the average velocity of the incoming and outgoing trajectories, $(v_0+v_1)/2$, where v_1 is the projectile velocity after collision. If the velocity difference of the incoming and outgoing trajectories is not taken into account, the Oen-Robinson theory gives a result that the

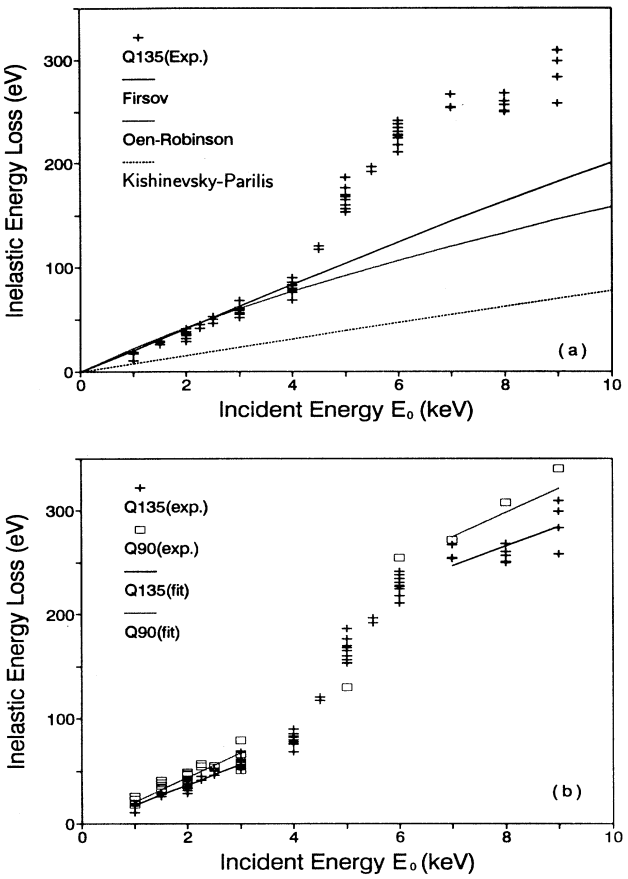

FIG. 7. (a) Inelastic energy loss of Ne^+-Cu at 135° scattering as a function of incident energy. Comparisons of the experimental results with that of the theoretical results calculated using the Firsov (modified), Kishinevsky-Parilis, and Oen-Robinson formulas. (b) The fitted inelastic energy loss using our model for both 135° and 90° scattering in comparison with that of the experimental results.

inelastic energy loss of 135° scattering is larger than that of 90° scattering, similar to that given by the original Firsov formula. The experimental results show that this is not the case [Fig. 3(a) and Sec. III A 5 (3)]. The Kishinevsky-Parilis formula gives a result which agrees qualitatively with that of the experiment.

However, the discrepancy between the experiments and these theories is quite large above 4 keV. These results suggested that the statistical treatment of the mean excitation of electrons in the collisions is not appropriate for the present cases. The threshold behavior in the inelastic losses indicates that inner-shell excitation might be taking place.

Inner-shell electron promotion models[35,39,40] can explain the discrete change in the inelastic energy loss, but the energy lost in these processes will only reach about 100 eV even considering the formation of $Ne(2s^{-2})$ states.[45] Further, the energy losses in such inner-shell promotion should be zero before it happens and constant after it finishes.

We suggest that the inelastic energy losses in a general collision process can be expressed as

$$Q_{\text{total}}=Q_e+Q_{\text{inner}} , \tag{14}$$

where Q_e is the energy lost in the mean electron excitation of collision partners along the trajectories, and Q_{inner} is the energy lost in pure inner-shell excitation processes. It is expected that the Q_e is related to the projectile trajectory, projectile velocity, and mean electron densities of both projectile and target atoms in their overlapping region. Q_{inner} is related to the overlapping of the atomic orbits of the colliding pair, and so is mainly related to the distance of closest approach during the encounter. It will therefore show a threshold-type behavior as a function of the internuclear distance between the collision partners—the inner-shell excitation energy loss is zero below a threshold distance, rising from a value near zero at the threshold, increasing sharply above the threshold, and eventually reaching a constant value when the internuclear distance exceeds the effective range.[39] Since the distance of closest approach is a function of scattering angle at constant incident energy, the threshold energy is expected to be a function of the scattering angle.

The energy lost in the mean electron excitation process during passage through a small length dL along the projectile trajectory can be expressed in differential form[16,17] as

$$dQ_e=Cv dL , \tag{15}$$

where v is the particle velocity in units of the Bohr velocity v_B, and C is a coefficient, which could depend on the electronic densities of projectile and target material in their overlapping region and may depend on particle velocity. In the case where the trajectory length is not very long, so that the spatial variation of the velocity along the trajectory could be neglected—and, for a further approximation, assuming that C is proportional to v^s—for this simplest case we obtain

$$Q_e=C_0 L v^n , \tag{16}$$

where $n+1+s$, C_0 is a constant, and L is the trajectory length which is also a function of incident energy and scattering geometry. In the case of large scattering angles, the scattered velocity will be very different from that along the incident trajectory. Therefore, we divide the trajectory into two parts: incoming and outgoing trajectories. The total inelastic energy loss could be expressed as

$$Q_{\text{total}}=C_0 L_{\text{in}} v_0^n+Q_{\text{inner}}+C_0 L_{\text{out}} v_1^n , \tag{17}$$

where L_{in} and L_{out} are the path lengths of the incoming and outgoing trajectories, respectively. v_0 and v_1 are the incident and scattered particle velocities in units of Bohr velocity v_B.

In order to calculate the trajectory length, a cutoff height H_0 has to be defined relative to the topmost ion cores of the surface. Here we chose 1.3 Å for the Cu(100) surface, similar to that used by others for the Ni(110) surface.[16,17] If the distance of closest approach r_0 is known

for a single collision in a given scattering geometry, L_{in} and L_{out} could be expressed approximately by

$$L_{in}=(H_0-r_0)/\sin\psi$$

and (18)

$$L_{out}=(H_0-r_0)/\sin(\theta-\psi)\ ,$$

where ψ is the incident angle of the projectile relative to target surface, and θ is the laboratory scattering angle. From our experimental results, it is clear that the threshold energy is above 3 keV and the inner-shell excitation was complete above 7 keV for both scattering angles. Therefore, we assume Q_{inner} can be expressed as

$$Q_{inner}=0 \quad \text{if } E_0 \leq 3 \text{ keV}\ , \tag{19a}$$

$$Q_{inner}=Q_0 \quad \text{if } E_0 \geq 7 \text{ keV} \tag{19b}$$

for both scattering angles used in the experiments, where Q_0 is constant for a certain inner-shell excitation process.

Three parameters n, Q_0, and C_0 in the above expressions are used to fit experimental inelastic energy-loss data as a function of incident energy of Ne^+-Cu for 90° and 135° scatterings simultaneously. The parameters which best fit the experimental results are found to be $n=1.8$, $Q_0=112$ eV, and $C=3311.0$ eV/Å.

Figure 7(b) shows the fitted results of Q_{total} in the incident energy region above and below the inner-shell excitation for both 135° and 90° scatterings. The agreement between theory and experiment is satisfactory.

Using the parameters obtained above, Q_e can be obtained by

$$Q_e=C_0L_{in}V_0^n+C_0L_{out}V_1^n\ . \tag{20}$$

The results are shown in Figs. 8(a) and 8(b) for 135° and 90°, respectively. The inelastic energy loss calculated using Firsov (modified as discussed above), Kishinevsky-Parilis, and Oen-Robinson formulas are also shown for comparisons. There is a better agreement between the modified Firsov model and the fitted results in the case of Ne^+-Cu scattering.

The inelastic energy loss obtained by reversing the trajectory can be explained using the model. At a fixed scattering angle of 135°, the 45° and 90° incidence situations are simply a reversing of the incoming and outgoing trajectories. The trajectory length is about the same for these two cases, and therefore energy losses are about the same. The small difference [Fig. 3(b)] is caused by the difference in ion velocity along the unequal incoming and outgoing trajectories. The velocity of 45° incident ions is higher on the longer incoming trajectory and lower on the shorter outgoing trajectory, while that of 90° incident ions is higher on the shorter incoming trajectory and lower on the longer outgoing trajectory. This could therefore lead to a slightly larger energy loss Q_e in the 45° incident case than that of the 90° case. Since the incident energy and the scattering angle are the same for these two cases, Q_{inner} would remain the same. The total energy loss therefore follows the change in Q_e; that is, the energy loss is slightly larger for the 45° incident case than that for the 90° one. This agrees quite well with the experimental results.

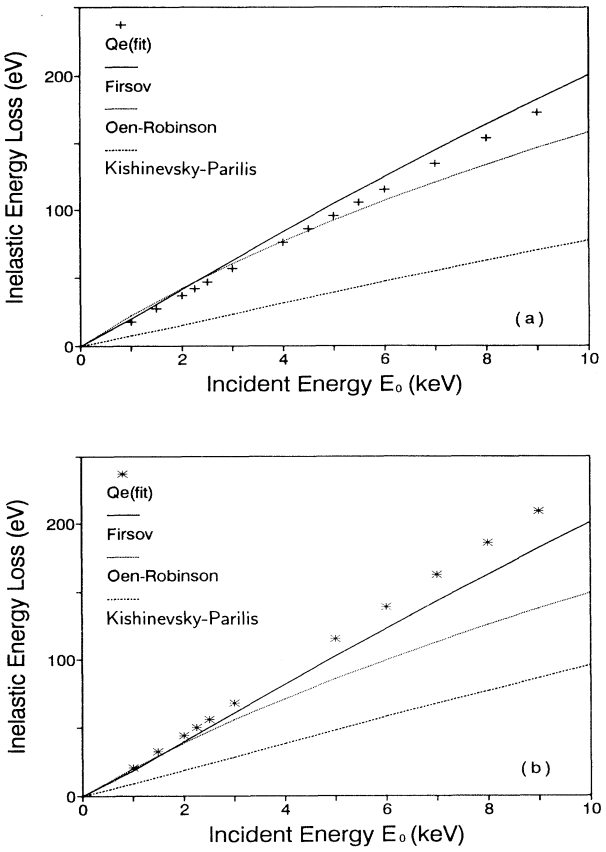

FIG. 8. The energy lost in the mean electron excitation Q_e obtained from our model in comparison with that calculated using Firsov (modified), Kishinevsky-Parilis, and Oen-Robinson formulas for (a) 135° scattering and (b) 90° scattering.

The energy lost in the inner-shell excitation Q_{inner} can be extracted by subtracting Q_e from the inelastic energy loss obtained from the experiments. Figure 9(a) shows the results of Ne^+-Cu collisions for both 135° and 90° angle scatterings as a function of incident energy. The inner-shell excitation process causes an energy loss which is zero below 3 keV and rises from zero at about 3–4 keV, begins to increase sharply in the region 4–6 keV, and reaches a constant value above 6 keV for 135° scattering. At 5-keV incidence, Q_{inner} is close to the constant value Q_0 for 135° scattering, while for 90° scattering Q_{inner} is slightly larger than zero at 5-keV incidence. This indicates that the threshold energy for 90° scattering is slightly higher than that of 135° scattering. The results of Q_{inner} versus incident energy E_0 can be converted into those of Q_{inner} versus the internuclear distance r_0, since the distance of closest approach r_0 can be calculated for a given incident energy and scattering angle using the universal potential or Molière potential. Figure 9(b) shows Q_{inner} as a function of closest approach distance r_0 (using the universal potential) for both 135° and 90° scatterings. The threshold energy somewhere between 3 and 4 keV for 135° scattering corresponds to a threshold

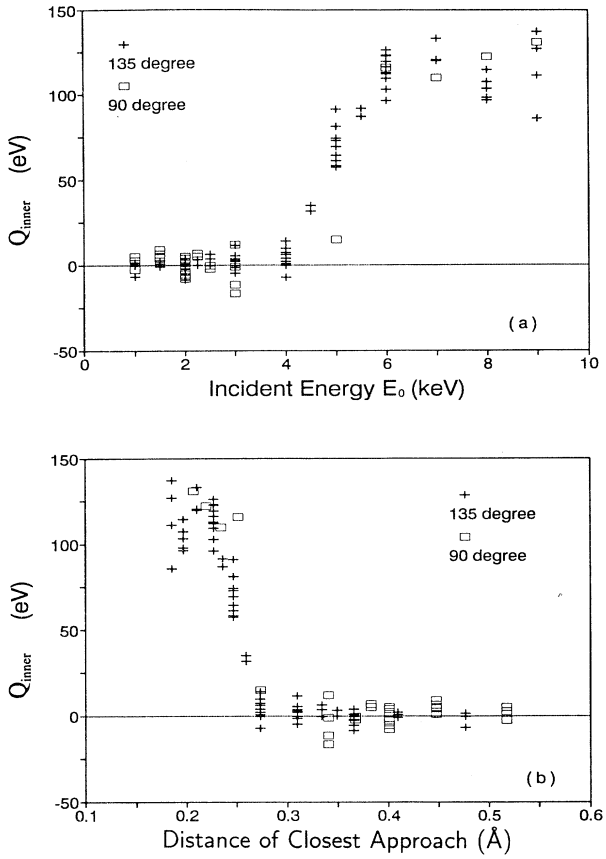

FIG. 9. The energy lost in the inner-shell excitation Q_{inner} of Ne^+-Cu scattering for both 135° and 90° scattering (a) as a function of incident energy (b) as a function of the closest approach distance r_0.

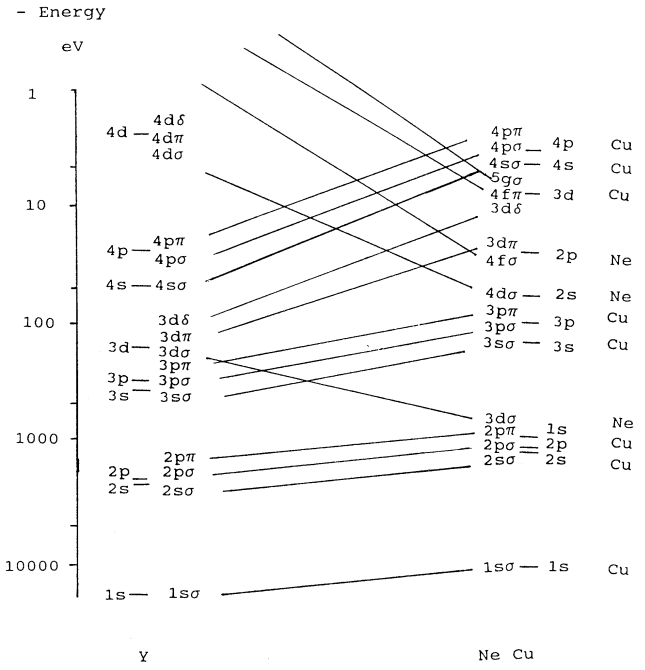

FIG. 10. The diabatic MO correlation diagrams of Ne-Cu constructed following Barat-Lichten rules (Ref. 39).

internuclear distance between 0.31 and 0.27 Å, i.e.; $r_c(135°)$ is around 0.29 Å. The threshold energy somewhere between 3 and 5 keV for 90° scattering corresponds to a threshold between 0.34 and 0.27 Å; i.e., $r_c(90°)$ is around 0.305 Å. This suggests that the threshold r_c for the inner-shell electron excitation is roughly the same for both 135° and 90° scatterings. This threshold distance of around 0.29–0.3 Å agrees quite well with the threshold or the sharp increase in ion fraction for Ne^+-Cu at 90° angle scattering[45] and 30° angle scattering,[41,42] as well as the threshold for the sharp increase in peak displacements of Ne^+-Cu at 90° angle scattering[45] and 164° angle scattering.[44] The distance of closest approach of 0.29 Å is about half the sum of the related radius of electron orbitals in the colliding particle (Ne 2*s* and Cu 3*p*), which is consistent with the results obtained in the ion-gas collision experiments for various projectiles and targets.[33,39]

To understand the inner-shell electron excitation processes, electron promotion models[35,39] are often used. The diabatic molecular-orbital (MO) correlation diagrams of Ne-Cu, which can be constructed following the Barat-Lichten rules,[39] have been given by Buck *et al.*[45] and also show in Fig. 10 for convenience. From the diagram, it can be seen that the Ne 2*p*, Ne 2*s*, (inner-shell) and Cu 3*d* (outer-shell) orbitals are strongly promoted to those of MO's of the same symmetry. Buck *et al.*[45] suggested the possibility of two Ne 2*s* excitations during the close Ne-Cu collisions. The energy loss would be up to ~ 106 eV$+\varepsilon$, corresponding to Ne($2s^{-2}$) states and two electrons with energy ε above the Fermi level. The inelastic energy lost in the inner-shell excitation process obtained in our study is a constant of ~ 112 eV for both scattering angles, in excellent agreement with the energy needed to form Ne($2s^{-2}$) states.

The formation of Ne doubly charged ions is observed in our experiments, as shown in Fig. 6(b). The threshold energy for the Ne^{2+} yield is about 4 keV at the 135° angle scattering, which corresponds to a closest approach distance $r_c' \sim 0.27$ Å, slightly smaller than that of the inelastic energy loss and scattered Ne singly charged ion yield. These results suggest that the following charge-exchange processes might occur in Ne^+-Cu surface collisions.

A. Incoming trajectory

In the incoming trajectory the incident Ne^+ ions could experience the usual velocity-dependent Auger and resonance neutralization by interactions with the Cu surface; i.e., they might undergo the following changes:

$$Ne^+ \rightarrow Ne^0 \text{ (Auger neutralization)},$$

$$Ne^+ \rightarrow Ne^* \text{ (resonance neutralization)},$$

or

$$Ne^+ \rightarrow Ne^+ \text{ (survival ions)}.$$

B. Close atomic encounter

According to the promotion models[39] and the diabatic MO correlation diagrams of the Ne-Cu system shown in Fig. 10, the Ne $2p$ and Ne $2s$ electron excitations become possible if the internuclear distance between Ne and Cu is shorter than the critical value r_c (~ 0.29 Å) during the close atomic encounter. If it is a one-electron excitation process, the Ne states formed in the incoming trajectory may undergo the following changes:

$$Ne^0 \rightarrow Ne^*, \quad Ne^* \rightarrow Ne^{**}, \quad \text{and} \quad Ne^+ \rightarrow Ne^{+*} .$$

If it is a two-electron excitation process, Ne particles may undergo the following changes:

$$Ne^0 \rightarrow Ne^{**}, \quad Ne^* \rightarrow Ne^{***} \quad \text{and} \quad Ne^+ \rightarrow Ne^{+**} .$$

C. Outgoing trajectory

Besides the usually Auger neutralization, resonance neutralization and ionization, and the deexcitation process which could happen to the scattered Ne particles in the outgoing trajectory, some of the Ne excited particles surviving deexcitation could remain in an excited state and autoionize further away from the surface, owing to its longer lifetime:[27,28]

$$Ne^{**} \rightarrow Ne^+ + e^- .$$

The autoionized Ne ions have a higher probability of escape from neutralization, since they occur far away from the surface. Therefore an enhanced Ne^+ ion yield [Fig. 6(a)] could be observed at about the same threshold as that for the sharp increase in the inelastic energy loss caused by inner-shell electron excitations.

Some of the Ne excited states formed by the two-electron excitation process could also have probabilities to autoionize into Ne^{2+} states, such as

$$Ne^{+**} \rightarrow Ne^{2+} + e^- .$$

The experimental fact that the threshold distance r_c' for observation of Ne^{2+} is shorter than that of Ne^+ ions may be caused for two reasons.

(i) The one-electron excitation process prevails when the internuclear distance just reaches the critical value r_c.

(ii) Ne^{2+} has a higher probability to transfer to lower charged states. The evidence of such a process was observed, and the results were shown in Fig. 6(c). The ratio between Ne^{2+} and Ne^+ yields is about 0.1 for the first-layer scattering and only 0.05 for the first two layers, indicating the larger charge-transfer probability from Ne^{2+} to that of Ne^+ or Ne^0. The remarkably rapid neutralization of highly charged particles to lower charge states when they interact with solids or surfaces has been observed for He, Ar, N, and Ne particles in other studies.[52,53]

As the internuclear distance further decreases, more and more Ne particles could be excited during the close encounter, and thus induce the sharp increase in the inelastic energy loss, and the yield of scattered Ne^+ and Ne^{2+} as shown in Figs. 5, 6(a), and 6(b), respectively. Different excitation combinations, such as excitations of one electron in Ne $2p$ and one electron in Ne $2s$, and excitations of one electron or two Ne $2s$ electrons, could occur, and this could induce several distinct peaks in the scattering spectrum. Because the energy difference between Ne $2p$ and $2s$ levels and the energy difference between excitation of one electron and that of two electrons in the $2p$ and $2s$ level are small (less than 50 eV in all cases), these peaks are not resolved. However, a broader increase in the peak width of the scattered ion energy spectrum has been observed in the effective range[39] where inner-shell excitation occurs, and will be discussed below. As shown in Fig. 9, the constant Q_{inner} value is reached when the internuclear distance between Ne and Cu is shorter than ~ 0.23 Å, so the effective range[39] (interaction range) of this inner-shell electron excitation process is

$$\lambda \approx (r_c - 0.23) \text{ Å} \approx (0.29 - 0.23) \text{ Å} \approx 0.2 r_c , \tag{21}$$

in excellent agreement with the results obtained in ion-gas collisions.[39] The Q_{inner} value of about 112 eV obtained in our study, in comparison with the energy needed to excite two Ne $2s$ electrons, indicates that the majority of the detected Ne^+ ions scattered from Cu surfaces result from Ne double-excited states with two Ne $2s$ vacancies at higher incident energies (above ~ 6 keV for 135° scattering angles, corresponding to the closest approach distance of about 0.23 Å). Detailed studies of the Ne $2s$ electron excitation probability for Ne^+ off various targets (Fe, Ni *et al.*), which is related to the swapping point[39] and various conditions, are reported elsewhere.[54]

The two-part inelastic energy-loss process is also reflected in the behavior of the peak width ΔE_{FWHM} (full width at half maximum) of the experimental spectrum as a function of incident energy, as shown in Fig. 11(a) for Ne^+-Cu scattering. The main feature in ΔE_{FWHM} is that of a gradual increase in 2–3-keV incident energy region, followed by a sudden increase above 4 keV and back to the gradual increase again at about 6 keV incident. This can be seen more clearly in Fig. 11(b)—variations in the ΔE_{FWHM} of one of the peaks corresponding to scattering from the Cu isotope as a function of incident energy. These two Cu isotope spectra were obtained by using two equal-width Gaussian peaks to fit the experimental spectrum. The fitting result is confirmed to be correct by the excellent agreement between the energy difference of the two Gaussian spectra with that calculated for Cu isotopes (natural isotope content in Cu samples). Figure 11 also shows that the threshold energy for the sharp increase in ΔE_{FWHM} is about the same as that observed in inelastic energy losses. As discussed above, in the effective range of the inner-shell process, the scattered Ne^+ ions experienced different one or two inner-shell electron excitation processes, which resulted in large discrete energy differences in the scattered ions and several unresolved peaks in the scattered ion energy spectrum. This therefore causes an increased width of the peak, in excellent agreement with the experimental results shown in Fig. 11. At about 6 keV, nearly all the scattered ions experienced the same two Ne $2s$ electron excitation processes and had about the same inner-shell inelastic energy loss; therefore the peak width went back to the extrapolated

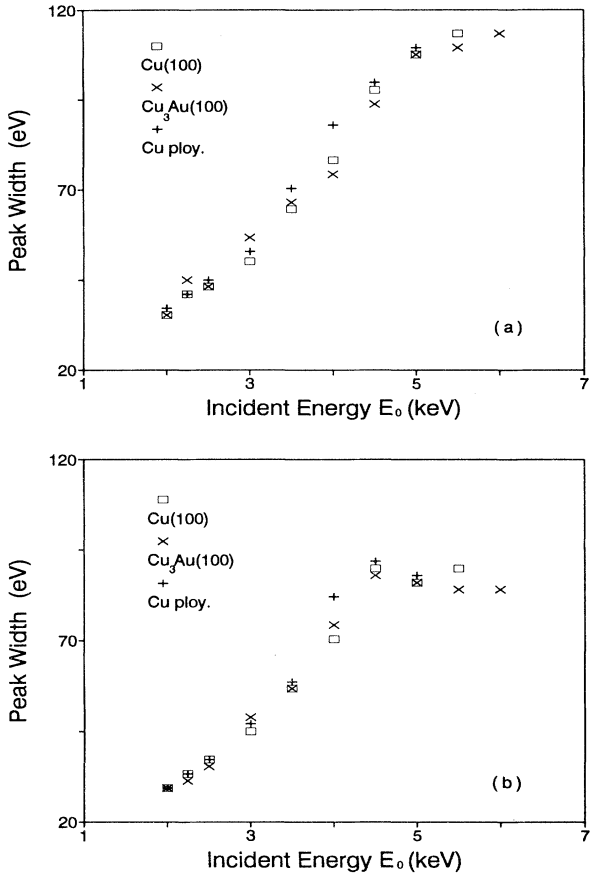

FIG. 11. The ΔE_{FWHM} (full width at half maximum) as a function of incident energy for Ne^+-Cu scattering at a 135° angle. (a) The ΔE_{FWHM} of experimental raw spectra. (b) The ΔE_{FWHM} for the peak corresponding to scattering from ^{63}Cu.

behavior of 2–3-keV incident energy region where no inner-shell excitation occurs.

The threshold for the Cu positive recoil ion is ~2 keV at a recoil angle 60°, which corresponds to Ne ions scattered at a angle of 46.75°. The corresponding threshold distance of closest approach is ~0.5 Å, larger than that associated with the Ne singly and doubly charged ions. The yield of the Cu positive recoil is determined by two processes: The ionization probability in the close encounter, and the survival probability of the ions in the outgoing trajectory. From the correlation diagram show in Fig. 10, one should expect Cu 3*d* outer-shell electron promotion to occur at a larger internuclear distance than that of Ne 2*p* and 2*s* electrons, as observed in the experiments. The survival probability of the Cu ions leaving the surface is expected to be a monotonically increasing function of ion velocity as given in Eq. (6). This combination of the two factors gives the Cu positive recoil yield a threshold-type shape as a function of incident energy: rising from a value near zero at the threshold, increasing sharply above the threshold, and then eventually decreasing the rate of increase at the incident energy increases, in good agreement with our experiments, as shown in Fig. 6(d). From Fig. 10, it can be seen that the energy lost in this process is only ~7 eV for one Cu 3*d* electron excitation. Although it is suggested that in general only rough, qualitative, and sometimes unreliable predictions can be made from the simple MO models[39] for the valence shell, the results obtained indicates that the prediction is valid for Cu 3*d* electrons for the Ne-Cu collision system.

One of the obvious differences between the diabatic MO correlation diagrams of Ne-Cu and Ne-Mg systems is the Ne 2*s* orbital. The Ne 2*s* level is strongly promoted via several crossings for the Ne-Cu system, as shown in Fig. 10, while for Ne-Mg system this is not the case.[29,45] The energy loss of about 45 eV observed in the Ne-Mg scattering[28] corresponds to excitation of the two Ne 2*p* electrons' excitation, in good agreement with the correlation diagram.[29,45] However, systematic experimental data about the inelastic energy loss as a function of incident energy are not available for the Ne^+-Mg case,[28] thus further comparison with Ne^+-Cu case is not able to be made at present. The difference in the excitation probability of Ne 2*p* electrons between Ne-Mg and Ne-Cu collision systems is related to the swapping point[39] of the Ne 2*p* level and the increase of target atomic number *Z*, and are discussed elsewhere.[54]

The inelastic energy-loss processes of the Na^+-Cu collisions can be understood using the same model proposed for Ne-Cu collisions. Since the energy losses in Q_e processes are related to the electron density of the collision particles, the trajectory length, and the velocity, which are about the same for Na^+-Cu and Ne^+-Cu at the same scattering geometry. Therefore the Q_e values should be about the same. The electron density in the Na^+ ions is slightly higher than that of the Ne^+, and thus may induce a slightly larger Q_e along the incoming and outgoing trajectories. The diabatic MO correlation diagram of Na-Cu is very similar to that of Ne-Cu except that the corresponding shell energy levels of the Na and the united atom (Zr) move toward lower energies. Thus we would expect a larger Q_{inner} value and a smaller internuclear distance for the inner-shell excitation processes.[39] The threshold internuclear distance observed from our experiments, corresponding to 4–4.5-keV incident energy at 135° scattering angle as shown in Fig. 4(a), is somewhere around 0.287–0.273 Å, in good agreement with the models. Doubly charged Na^{2+} was not observed; this may be caused by the high background in the spectra masking those Na^{2+} signals.[55,56]

The larger energy losses for Ne^+-Au collisions than for Ne^+-Cu at lower incident energies may be caused by the higher electron density in the Au atoms. At higher energies, the much stronger repulsive force from Au atoms may induce a slower increase of the inelastic energy loss as the incident energy increases. This may also be one of the reasons that inner-shell excitations were not observed in the energy region studied. This agrees with the results obtained from ion fraction and Auger electron spectroscopy experiments.[45] Detailed studies of the inelastic energy loss and charge-exchange process in Ne^+ scattering from Au and Au alloy surfaces are reported elsewhere.[57]

The results obtained from Ne^+-Cu, Na^+-Cu, and

Ne^+-Au scattering suggested that the inelastic energy loss is dependent on the particle trajectory, the velocity, the electron density of both projectile and target atoms, and the distance of closest approach in the scattering event. This study reveals that all Ne ions scattered from Cu atoms in the Cu or Cu alloy surface could experience a significant inner-shell electron excitation loss in addition to the mean electron excitation losses along the trajectories even in the low-energy region (below 9 keV). Large inelastic energy losses also exist in the Na^+-Cu and Ne^+-Au collisions. These results suggest that the usual assumption that the low-energy ion backscattering event from a clear metal surface is a pure elastic-scattering process may need further examinations, particularly at energies in the 5–10-keV region.

V. CONCLUSIONS

Inelastic energy losses in the Ne^+-Cu, Ne^+-Au, and Na^+-Cu collisions are large in the low-energy region (below 9 keV) at large scattering angles. The inelastic energy loss is independent of the target matrix for Ne^+-Cu collisions, but varies as a function of scattering angle. The model in which the inelastic energy loss in a general ion-surface collision is composed of the energy lost in a pure inner-shell electron excitation process and the energy lost in mean electron-hole pair excitations along the trajectories is in good agreement with the experimental results. The value of the energy lost in the inner-shell electron excitations for Ne^+-Cu collisions obtained in our study is about 112 eV, strongly supporting the proposition that two Ne $2s$ electrons are promoted to form the Ne($2s^{-2}$) excited states during the close atomic encounter.[45]

ACKNOWLEDGMENTS

The authors are grateful to Dr. Qing Yang for useful discussions and computer software support. The authors would like to thank Associate Professor D. J. O'Connor and Dr. B. V. King for useful discussions and kind help in the experiments. We would also like to thank C. Stellmaker, Dr. Y. Shen, P. Greig, and M. O'Neill for the help on some technical work.

[1]H. D. Hagstrum, Phys. Rev. **96**, 336 (1954).
[2]H. D. Hagstrum, in *Inelastic Ion-Surface Collisions,* edited by N. H. Tolk, J. C. Tully, W. Heiland, and C. W. White (Academic, New York, 1977), pp. 1–25.
[3]T. M. Buck, G. H. Wheatley, and L. K. Verheij, Surf. Sci. **90**, 635 (1979).
[4]R. J. MacDonald and P. J. Martin, Surf. Sci. **111**, L739 (1981).
[5]R. J. MacDonald, D. J. O'Connor, J. Wilson, and Y. G. Shen, Nucl. Instrum. Methods Phys. Res. Sect. B **33**, 446 (1988).
[6]G. Verbist, H. H. Brongersma, and J. T. Devreese, Nucl. Instrum. Methods Phys. Rev. Sect. B **64**, 572 (1992).
[7]A. L. Boers, Nucl. Instrum. Methods Phys. Res. Sect. B **4**, 98 (1984).
[8]D. P. Woodruff, Surf. Sci. **116**, L219 (1982).
[9]O. B. Firsov, Zh. Eksp. Teor. Fiz. **36**, 1517 (1959) [Sov. Phys. JETP **36**, 1076 (1959)].
[10]J. Lindhard and M. Scharff, Phys. Rev. **124**, 128 (1961).
[11]O. S. Oen and M. T. Robinson, Nucl. Instrum. Methods **132**, 647 (1976).
[12]L. M. Kishinevsky, Izv. Akad. Nauk SSSR Ser. Fiz. **26**, 1410 (1962) (see Ref. 14).
[13]L. M. Kishinevsky and E. S. Parilis, Izv. Akad. Nauk SSSR Ser. Fiz. **26**, 1409 (1962) (see Ref. 14).
[14]E. S. Parilis, L. M. Kishinevsky, N. Yu. Turaev, B. E. Baklitzky, F. F. Umarov, V. Kh. Verleger, S. L. Nizhnaya, and I. S. Bitensky, *Atomic Collisions on Solid Surfaces* (North-Holland, Amsterdam, 1993), p. 18.
[15]P. M. Echenique, F. Flores, and R. H. Ritchie, in *Solid State Physics,* edited by H. E. Ehrenreich and D. Turnbull (Academic, New York, 1990), Vol. 43, p. 229.
[16]A. Narmann, W. Heiland, R. Monreal, F. Flores, and P. M. Echenique, Phys. Rev. B **44**, 2003 (1991).
[17]W. Heiland and A. Narmann, Nucl. Instrum. Methods Phys. Res. Sect. B **78**, 20 (1993).
[18]H. F. Helbig, P. J. Adelmann, A. C. Miller, and A. W. Czanderna, Nucl. Instrum. Methods **149**, 581 (1978).
[19]P. Pertrand and M. Ghalim, Phys. Scr. **T6**, 168 (1983).
[20]A. D. F. Kahn, D. J. O'Connor, and R. J. MacDonald, Surf. Sci. Lett. **262**, L83 (1992).
[21]F. Shoji, Y. Nakayama, K. Oura, and T. Hanawa, Nucl. Instrum. Methods Phys. Res. Sect. B **33**, 420 (1988).
[22]P. Bertrand, Nucl. Instrum. Methods **170**, 489 (1980).
[23]T. M. Buck, I. Stensgaard, and G. H. Wheatley, Nucl. Instrum. Methods **170**, 519 (1980).
[24]T. M. Buck, G. H. Wheatley, and D. P. Jackson, Nucl. Instrum. Methods Phys. Res. **218**, 257 (1983).
[25]D. P. Jackson, T. M. Buck, and G. H. Wheatley, Nucl. Instrum. Methods Phys. Res. Sect. B **2**, 440 (1984).
[26]R. J. MacDonald and D. J. O'Connor, Surf. Sci. **124**, 433 (1983).
[27]W. Heiland and E. Taglauer, in *Inelastic Ion-Surface Collisions* (Ref. 2), p. 27.
[28]O. Grizzi, M. Shi, H. Bu, J. W. Rabalais, and R. A. Baragiola, Phys. Rev. B **41**, 4789 (1990).
[29]G. Zampieri, F. Meier, and R. Baragiola, Phys. Rev. A **29**, 116 (1984).
[30]V. A. Esaulov, L. Guillemot, and S. Lacombe, Nucl. Instrum. Methods Phys. Res. Sect. B **90**, 305 (1994).
[31]F. Xu, N. Mandarino, A. Oliva, P. Zoccali, M. Camarca, and A. Bonanno, Nucl. Instrum. Methods Phys. Res. Sect. B **90**, 564 (1994).
[32]J. W. Rabalais, Jie-Nan Chen, R. Kumar, and M. Narayana, J. Chem. Phys. **83**, 6489 (1985).
[33]B. Fastrup, G. Hermann, and K. J. Smith, Phys. Rev. A **3**, 1591 (1971).
[34]A. K. Edwards and M. E. Rudd, Physical Review **170**, 140 (1968).
[35]U. Fano and W. Lichten, Phys. Rev. Lett. **14**, 627 (1965).
[36]R. Souda and M. Aono, Nucl. Instrum. Methods Phys. Res. Sect. B **15**, 114 (1986).
[37]R. Souda, T. Aizawa, C. Oshima, S. Otani, and Y. Ishizawa, Surf. Sci. **194**, L119 (1988).
[38]S. Tsuneyuki and M. Tsukda, Phys. Rev. B **34**, 5758 (1986).
[39]M. Barat and W. Lichten, Phys. Rev. A **6**, 211 (1972).
[40]W. Lichten, Phys. Rev. **131**, 229 (1963).
[41]S. B. Luitjens, A. J. Algra, and A. L. Boers, Surf. Sci. **80**, 566

(1979).
[42]S. B. Luitjens, A. J. Algra, E. P. Th. M. Suurmeijer, and A. L. Boers, Surf. Sci. **99**, 631 (1980).
[43]E. Van de Riet, J. B. J. Smeets, J. M. Fluit, and A. Niehaus, Surf. Sci. **214**, 111 (1989).
[44]Th. Fauster, Vacuum **38**, 129 (1988).
[45]T. M. Buck, W. E. Wallace, R. A. Baragiola, G. H. Weatley, J. B. Rothman, R. J. Gorte, and J. G. Tittensor, Phys. Rev. B **48**, 774 (1993).
[46]R. Souda, M. Aono, C. Oshima, S. Otani, and Y. Ishizawa, Surf. Sci. **128**, L236 (1983).
[47]Q. Yang, Nucl. Instrum. Methods Phys. Res. Sect. B **90**, 602 (1994).
[48]H. Niehus, W. Heiland, and E. Taglauer, Surf. Sci. Rep. **17**, 213 (1993).
[49]T. W. Rusch and R. L. Erickson, J. Vac. Sci. Technol. **13**, 374 (1976).
[50]J. W. Rabalais, CRC Crit. Rev. **14**, 319 (1988).
[51]W. N. Lennard and H. Geissel, in *Interaction of Charged Particles with Solids and Surfaces,* edited by A. Gras-Marti, H. M. Urbassek, N. R. Arista, and F. Flores (Plenum, New York, 1991), p. 347.
[52]G. E. Chapman, D. J. O'Conner, and R. J. MacDonald, Nucl. Instrum. Methods Phys. Res. Sect. B **21**, 20 (1987).
[53]F. W. Mayer, S. H. Overbury, C. C. Havener, P. A. Zeijlmans van Ennichoven, and O. M. Zehner, Phys. Rev. Lett. **67**, 723 (1991).
[54]T. Li and R. J. MacDonald (unpublished).
[55]A. J. Algra, E. V. Loenen, E. P. Th. M. Suurmeijer, and A. L. Boers, Radiat. Eff. **60**, 173 (1982).
[56]R. Zimny, Surf. Sci. **233**, 333 (1990).
[57]T. Li and R. J. MacDonald (unpublished).